Linear volcanic segments in the central Sunda Arc, Indonesia, identified using Hough Transform analysis: Implications for arc lithosphere control upon volcano distribution

Adam Pacey[1,†], Colin G. Macpherson[1,*], Ken J. W. McCaffrey[1]

1 Department of Earth Sciences, University of Durham, Durham, DH1 3LE, UK

† Now at: Department of Earth Science & Engineering, Imperial College London, South Kensington, London SW7 2AZ, UK

* Corresponding author:

colin.macpherson@durham.ac.uk

Tel: +44 (0)191 334 2283

Fax: +44 (0)191 334 2301

Revised version returned to:

Earth and Planetary Science Letters

25 January 2013

Abstract

Hough Transform analysis is used as an objective means to constrain volcano distribution in the central Sunda Arc, Indonesia. Most volcanoes in the arc define four en echelon, linear segments, each of 500 to 700 km length. Javan volcanoes that do not lie on these segments either (i) formed at an early stage in the history of the arc and erupted products that are petrologically and geochemically distinct from typical arc magma, or (ii) lie along other mapped structures.

The en echelon distribution of volcanoes in the central Sunda Arc is best explained as originating from two possible sources. First, interaction with the subducting Indo-Australian Plate may induce stress in the arc lithosphere generating pathways for magma to exploit. Second, downward flexure of the arc lithosphere, as a result of mantle flow or loading by the arc, would also establish arc-normal tension towards the base of the lithosphere, where magma is supplied to volcanic systems.

To the west and east of the central Sunda Arc deviations from the distribution of long, en echelon, linear segments can be understood as responses to specific stress fields in the arc lithosphere of Sumatra and eastern Nusa Tenggara, respectively. Control of volcano distribution by arc lithosphere explains why there are large variations in the depth from volcanoes to the zone of slab seismicity in the central Sunda Arc, where there is little variation in slab geometry or the rate of plate convergence.

Keywords

Sunda Arc, volcano, segmentation, stress, lithosphere, Hough Transform analysis

1. Introduction

The overall curvature of many subduction zones is immediately apparent and the term “island arc” betrays the common assumption that subduction zone magmatism occurs in curved zones. This assumption can be expressed by approximating island arcs as segments of small circles on the surface of a sphere (England et al., 2004). Such treatments have been employed to relate the location of arc volcanoes to their vertical separation from the slab (in fact, the depth to seismicity in the slab) and require the primary control on the locus of magmatism to lie either within the subducted slab or the mantle wedge (Syracuse and Abers, 2006; Grove et al., 2009; England and Katz, 2010).

The concept of curved arcs ignores longstanding observations that magmatism in many subduction systems occurs as segments of linearly arranged volcanic centres (Carr et al., 1973; Stoiber and Carr, 1973; Marsh, 1979; Ranneft, 1979; Hughes et al., 1980). Further evidence for this distribution comes from the close relationship between magmatism and large scale, arc-parallel fabrics in some arcs (Buckart and Self, 1985; Bellier and Sébrier, 1994; Tosdal and Richards 2001; Bolge et al., 2009). Similarly, exposures of deep arc crust or mantle often reveal elongation of magmatic intrusions sub-parallel to the inferred trend of the arc (Tikoff and Teyssier, 1992; Rivera and Pardo, 2004; Bouilhol et al., 2010).

The Sunda Arc runs through Indonesia from Sumatra to Flores (Fig. 1) and provides an important test for models of volcano distribution for several reasons. First, Sunda has hosted abundant historic volcanic activity. Second, the vast majority of volcanoes in the arc are subaerial from base to cone and, therefore, can be readily identified through a combination of local mapping and satellite imagery. Third, there are significant changes in the stress regime along the length of the arc. To the west, highly oblique convergence causes significant strain partitioning associated with the Great Sumatran Fault (Barber et al., 2005) and to the east, the arc has collided with Australian continental lithosphere (Harris et al., 2009; Fig. 1). These changes in geodynamics allow the influence of the upper plate to be further evaluated by comparison of different arc segments. Finally, much of the Sunda Arc has proved difficult to accommodate in models that try to relate volcano distribution to the depth to the subducted slab. It has, however, previously been proposed as a site where a linear model may be more appropriate for understanding volcano distribution (Ranneft, 1979).

We apply an objective line-fitting, image analysis protocol; the Hough Transform, to explore the distribution of volcanoes in the central Sunda Arc from Java to central Flores. We focus on this section because of the complicating influences of the Great Sumatran Fault and the arc-continent collision to the west and east, respectively. Volcano distribution in the central Sunda Arc is best described as linear segments, or great circles on a sphere, rather than following small circles. We discuss the orientation of these segments and deviations from linear distribution both within our study area and beyond its eastern and western extremities. We conclude that the stress field in the Sunda Arc lithosphere is the primary control on the distribution of its volcanoes.

2. The Sunda Arc

The Sunda Arc stretches from the NW end of Sumatra to Java, then through Nusa Tenggara as far as Flores in the east and is part of the plate margin where the Indo-Australian Plate is subducted beneath Eurasia (Fig. 1). Indian Ocean lithosphere is subducted beneath most of the arc but Australia has collided with, and perhaps impeded subduction in, parts of the arc east of Flores (Audley-Charles, 2004; Harris et al., 2009). Motion of the Indo-Australia Plate varies from 63 mm/yr N14° with slight dextral obliquity south of the Sunda Strait, to perpendicular convergence of 67 mm/yr N14° south of Java to slightly obliquity, but in the opposite sense, at 70 mm/yr N13° south of Bali (Fig. 2; Simons et al., 2007). The margin's curvature, particularly around the Sunda Strait, leads to strong strain partitioning of dextral shear at Sumatra and neutral, or possibly even sinistral, shear through Java and Nusa Tenggara (McCaffrey, 1996). The dip of the slab remains relatively constant from the Sunda Strait (49°) to the Australian collision (46°; Syracuse and Abers, 2006), although tomographic evidence suggests that a slab hole may exist beneath east Java (Widiyantoro et al., 2011). The current Sunda Arc is largely a Quaternary feature in Java and Nusa Tenggara. These island groups are the focus of this work and their development is described in more detail below.

2.1. Java

Recently, the basement to much of Java has been recognised as continental fragments derived from the Australian margin of Gondwana that were accreted to the Sundaland margin in two stages during the Cretaceous (Smyth et al., 2007; Granath et al., 2011; Hall, 2011 and 2012). The first of these was accreted at the Billiton lineament around 115 to 110 Ma and now forms SW Borneo and western Java (block 2 in Fig. 1). A suture, composed of the same ophiolitic material seen in the Meratus Mountains of SE Borneo, separates the West Java Block from the East Java – West Sulawesi Block that may, itself, be comprised of several smaller fragments (block 3 in Fig. 1). This was accreted at about 90 Ma, probably around the same time as the Woyla Arc collided with Sumatra (Hall 2012).

Subduction then terminated around most of Sundaland until the Eocene. Thus, the basement of Java changes from the SW Borneo - West Java block in the west, through the Meratus Suture in central Java to the East Java – West Sulawesi Block in the east. These terranes were then covered by Cenozoic rocks of shallow water carbonate or clastic character over the Sunda shelf and volcaniclastic and deeper marine deposits further south. The volcaniclastic components originated in a Palaeogene Arc to the south of Java constructed upon continental basement (Clements et al., 2009). Volcanism then once again ceased and this Palaeogene arc was thrust northwards during the Late Miocene or Pliocene, where parts of it are preserved as the Southern Mountains (Fig. 2). The thrusting also uplifted Neogene sediments to the north of this arc as they were folded against the Sunda shelf, producing most of the land now exposed in central and eastern Java (Clements et al., 2009; Lunt et al., 2009).

Modern Sunda Arc volcanoes developed during the Quaternary and are constructed upon basement created by the processes described above. In West Java the arc is notable for its “broadening”, for example Tankuban Prahu lies approximately 80 km further from the Java Trench than volcanoes to its southwest (Fig. 2). This results in significant changes in the depth to the slab along the length of the island (Syracuse and Abers, 2006). Quaternary volcanism in Java has mainly generated basaltic andesite to andesite effusive and explosive products (Whitford, 1975). Extinct, Quaternary volcanoes that produced highly potassic, including leucititic, lavas lie to the north of the large mafic-intermediate stratovolcanoes (Foden and Varne, 1980; Leterrier et al., 1990; Edwards et al., 1991 and 1994).

2.2. Nusa Tenggara

Basement of Nusa Tenggara is less well known than Java because of less exposure and greater challenges to access. Furthermore, considerable portions of these islands are blanketed by Quaternary volcanic deposits. The island of Sumba is a forearc section, uplifted where Australian continental lithosphere has entered the trench (Harris et al., 2009, Fig. 1). Rigg and Hall (2011) interpret Sumba as part of the East Java – West Sulawesi Block that was accreted to Sundaland in the Cretaceous (Fig. 1). Other parts of Nusa Tenggara could be constructed on similar basement. Further east Nusa Tenggara may include different blocks of Gondwana-derived lithosphere, accreted at a later date and/or newly formed arc crust representing subduction products formed as the Java Trench propagated eastward in response to a phase of rapid slab rollback initiated at around 15 Ma (Spakman and Hall, 2010).

3. Methods

Previous studies have noted volcanoes distributed in linear segments in several arcs (Marsh, 1979; Ranneft, 1979; Hughes et al., 1980; Bolge et al., 2009 and references therein). Rather than “eyeballing” alignments we sought an objective method to identify such arrangement of volcanic structures. We considered multiscale trend analysis, in which a dataset is split into numerous smaller linear segments (Zaliapin et al., 2004), and random sample consensus, in which linear trends can be discovered in noisy datasets (Fischler and Bolles, 1981). However, these methods were ultimately rejected as they are not able to identify overlapping linear features, such as en echelon systems.

Volcanic arcs are already recognised as elongate arrangements of volcanic centres. Therefore, the aim of this study is to determine whether these centres are better modelled as small circles or great circles on a spherical surface i.e. are individual segments arcuate or linear. The Hough Transform method provides the most appropriate tool for this purpose.

3.1. The Hough Transform

The Hough Transform is applied to images to recognise geometric features that can be expressed mathematically, in this case lines. Modern applications are widespread, largely in physics and computer vision technology; however the technique has received relatively little application as a spatial analysis tool to detect geological structures (Wang and Howarth, 1990; Sæther et al., 1994; Karnieli et al., 1996; Cooper, 2006a and b; Yamaji et al., 2006; Jenkins et al., 2008). Some attempts have been made to identify volcanic alignment, mainly in monogenetic volcanic fields (Wadge and Cross, 1988; Connor, 1990; Connor et al., 1992). It is beyond the scope of this paper to present a detailed description of the mathematical concepts behind the Hough Transform, for which the reader is directed to Dunda and Hart (1971), Hart (2009) and references therein. A simple qualitative explanation of its use to recognise alignment is given below.

Any straight line in an image can be defined uniquely by two parameters related to the normal that passes through the origin of a Cartesian grid system (Fig. 3). The length of the normal is ρ while θ is the angle it makes with the x-axis. For each point in the image, values of ρ and θ are determined for straight lines with azimuths from 0° to 359° (Fig. 3a-b). A plot of ρ versus θ produces a sinusoidal curve (Fig. 3c) for each point. This is repeated for all points. The sine curves for points which are aligned will include the same coupled ρ - θ values because the normal will occur in the analysis of each point (e.g. normal 1 in Fig. 3a and normal 4 in Fig. 3b). Thus, intersection of sine curves in the ρ - θ plot identifies alignment (Fig. 3c). For images containing multiple possible alignments, a threshold value is defined, as a percentage of the highest frequency ρ - θ couple, to identify which further high frequency couples are either picked as potential alignments or disregarded. The ρ – θ values of the recurring normals are then used to draw alignments back on the original image.

A map of Sunda Arc volcanic centres was produced as a greyscale image file in UTM projection (see below) to ensure equal x and y scales. Initially, each volcanic centre was represented by a circle of uniform size (Fig. 4a). A script was then constructed, exploiting in-built Hough Transform functions in MATLAB®, to perform the analysis on the image. The script is essentially composed of three components; the first produces a ρ – θ parameter space plot, the second highlights and picks the highest frequency peaks from this plot, and the third projects the corresponding lines back onto the greyscale image. It was necessary to specify two values manually. First, the minimum line length acceptable was set such that lines which only connected three or less data points were not accepted as significant alignments. Second, the maximum gap value was set such that lines could connect between volcanoes separated by ~100 km, which equates to 2-3 times the average separation of volcanoes in the arc.

A second map of centres was explored in which volcanoes had non-uniform size. Each volcano was scaled to a circle three quarters of the diameter at its base, as determined from geological maps and satellite images (Fig. 4b). This approach effectively weights the analysis toward larger volcanic systems. It also allows projection of linear trends between structures, even if their exact geometric centres are not aligned. This accommodates the fact that a volcanic structure may not lie directly above the main feeding conduit at depth. A three-quarter diameter scaling was chosen because circles scaled to the full size of centres would have resulted in overlap of many structures that clearly originate from different volcanic systems.

3.2. Volcano location database

The digital elevation model used to identify volcanic features is 3 arc second (~90 m) resolution NASA SRTM, version 4 of Jarvis et al. (2008) projected into UTM (Fig. 2). Great circles describe straight lines on gnomonic map projections. However, the area studied lies close to, and trends sub-parallel to, the equator therefore a UTM projection provides a suitable approximation in this case, such that any straight lines identified represent great circles.

A distribution dataset was created by plotting the locations of all volcanic centres identified on SRTM and was verified by reference to published geological maps (see Supplementary Material A). Many, but not all, of these centres are documented in the Smithsonian Global Volcanism Program (Siebert and Simkin, 2002). Such cross-referencing ensured that the centres identified are real volcanic features of the current arc. Many small topographic features, typically of 1-3 km diameter, remain ambiguous while others are clearly secondary parasitic structures. Thus, given the regional perspective of this study, volcanic structures with a basal diameter of <3 km are excluded.

All volcanic centres are recorded as a single discrete point/coordinate representing the underlying magmatic system. The geographic centres of volcanic cones/vents or summit craters, where these were discernible, were picked. If several small craters/conduits were observed on top of a single larger structure, an average position was chosen. The locations of all geologically validated volcanic centres from the Sunda Strait to central Flores are shown in Fig. 2 and listed in Supplementary Material B.

Some alignment of centres is immediately apparent but it is also clear that several lie north of the main arc front (yellow triangles in Fig. 2). In Java, these centres are older than the main arc (Letterier et al., 1990) and have erupted highly potassic lavas (Fig. 5). Gunung Muriah, its subsidiary cone Genuk, in central Java along with the Ringgit-Beser complex and Gunung Lurus in east Java all lie close to the northern coast of Java and erupted potassic and ultrapotassic leucititic suites that resemble intra-plate magmatism from Australia (Edwards et al., 1991; Edwards et al., 1994). None have been historically active and some are clearly extinct. Gunung Lasem has a more arc-like calc-alkaline andesitic composition but is one of the oldest volcanic features in the arc and Leterrier et al. (1990) suggest that the location of this extinct centre, relative to the present margin, may not represent its position relative to the plate margin when it was active. Due to the distinction in age and/or origin of these centres we exclude them from the spatial analysis of the active arc.

Further to the east, Tambora, on the island of Sumbawa, and Sangeang Api, a small island NE of Sumbawa (Fig. 2), are also composed largely of potassic, nepheline normative trachybasalt-andesite (Foden and Varne, 1980; Foden, 1986). Therefore, these centres are also excluded from the distribution analysis. Sangenges volcano, in western Sumbawa, has erupted a silica undersaturated leucititic alkaline series but also produced typical, low-K, calc-alkaline andesites and dacites (Foden and Varne, 1980). For this reason Sangenges is included in the analysis.

4. Results

Several potential alignments of points were identified from the Hough Transform analysis of the uniform and weighted datasets (Fig. 4a and b). The length and number of points incorporated in each of these varies and several points are included in more than one segment. We focus on only the six segments that were common to both the uniform and weighted approaches. For each of these a coefficient of determination (R^2) was calculated for the points lying closest to them, i.e. within the ellipses drawn on Fig. 4c.

The westernmost segment (R^2 = 0.947) incorporates the same, unique set of points in both approaches and so we consider that these define a valid geological feature. There are two possible segments through the easternmost data but, since there is negligible difference between them, we regard these as a single segment (R^2 = 0.774). In the central area there are three potential segments. The shortest of these has the lowest R^2 value (0.917) and all of its points can be accommodated in one of the other two possible segments in this region. A potential segment covers the whole central area but, while R^2 for this is high (0.958), it only propagated across the gap between points A and B because it has grazed the point at C (Fig. 4c). Terminating this segment manually at point A gives a better constrained, east central segment (R^2 = 0.974), which complements the potential west central segment with R^2 of 0.964 (Fig. 4d).

Thus, an initial attempt at objective definition of alignment identifies four segments (Fig. 4d). Firmer constraints on the validity of these as true arc segments can be obtained by accounting for; 1) the different size of each volcanic centre, and 2) the influence of local basement structures upon the location of some volcanoes.

To address the sizes of volcanic systems a weighted regression was performed in which the weighting factor applied to each data point was the base diameter measured from the SRTM data (as recorded in Supplementary Material B). This assumes the surface expression of a volcanic centre is proportional to the significance of its underlying system. All of the centres are of Quaternary age and lie at similar latitudes, experiencing similar climatic conditions. Precipitation is high and so there is an opportunity for mass loss through erosion and mass wasting. While a constant rate of erosion would lead to a greater proportional loss from smaller edifices, we anticipate that such differences will be negligible for centres above the cut-off diameter for the database (3 km). The greatest effect of this is to increase the R^2 value of the east segment, where a number of smaller volcanic centres are more scattered around the largest ones.

Local controls on distributions are suggested where volcanoes deviate systematically from the segments identified in Fig. 4d. This is particularly apparent at the overlap of the west and west central segments and in the middle of the west central segment, north of Merapi and Sumbing (centres shown as orange in Fig. 6). Geological mapping reveals that volcanoes in these areas coincide with several mesoscale structural features (10-100 km long) that cut through deformed Cenozoic basement and Quaternary deposits (Fig. 6). In the Bandung region, there are distinct structural 'grains' visible in the SRTM imagery sub-parallel to both the identified volcanic alignments (WNW - ESE) and the mapped basement mesoscale structures (NE – SW; Fig. 6b). Thus, several volcanoes appear to exploit extensional or strike-slip faults where the west and west central segments overlap. A study of basement structures in west Java by Carranza et al. (2008) also revealed numerous lineaments with similar trends to this grain. In central Java, Sundoro volcano and the Dieng Volcanic Complex trend northwest of Sumbing parallel to local lineaments (Fig. 2). Likewise, Merbabu, Telomoyo and Ungaran trend north-northwest of Merapi (Fig. 6a). The other outlying vent coinciding with mesoscale structure is the more unusual Pandan (Fig. 6c), which consists of a brecciated andesite plug of uncertain origin, emplaced across an apparent lateral offset in a Tertiary fold belt (Pringgoprawiro and Sukido, 1992).

We propose that the primary distribution of volcanism in the central Sunda Arc is four, en echelon linear segments, but that second order crustal mesoscale structures are also exploited to produce the overall observed distribution. This being the case, it is possible to remove such locally controlled vents (marked orange in Fig. 6a). Then, conducting the weighted regression analysis to account for vent size defines the four main volcanic segments with R^2 values ranging from 0.85 to 0.99 (Fig. 7).

5. Discussion

The central Sunda Arc does not fit well into recent global syntheses of arc geodynamics for two reasons. First, the volcano distribution is not well approximated by small circles, the fit to which England et al. (2004) quantified using the root mean square (RMS) of deviation. The RMS for Java (12) was one of the largest among the arcs examined (mean = 6.9 for 24 arcs). The "Bali/Lombok arc" (defined by Syracuse and Abers, 2006) deviates even further than Java from the systematics predicted by the generic model for "small circle" arcs (England and Katz, 2010). Second, Java displays the largest along strike variation in depth to slab of any arc (Syracuse and Abers, 2006).

RMS values for deviations from the best fit linear segment, or great circles (Fig. 7), in Java are 6.7 for the west segment, 6.1 for the west central segment and 7.5 for the east central segment. The linear segments could, instead, be fitted with similar RMS by small circles only slightly smaller than great circles. In this case, the improved fit might be attributed simply to the recognition of more segments. However, this would not eliminate the variation in depth to seismicity. Despite relatively constant dip and subduction velocity from Java to central Flores (Section 2) there are significant variations in the depth to seismicity both between and within the segments (Fig. 8). Thus, our observations question both of the premises used to invoke the control of volcano distribution originating at depth within subduction zones.

Instead, both the linearity of segments and the variation in depth-to-slab within, and between, segments are more consistent with volcano distribution being controlled by the arc lithosphere. Upper plate control is also suggested by the overlap between the west and west central, and between the west central and east central segments (Fig. 7). Such overlap of linear features is a common attribute of tectonic failure in brittle plates. In the following section we discuss mechanisms by which the arc lithosphere could control the central Sunda Arc volcano distribution.

5.1. Upper plate control on distribution of volcanoes in the central Sunda Arc

The earliest observations of linear arc segmentation invoked linear zones of melting at or close to the slab–wedge interface (Carr et al., 1973; Stoiber and Carr, 1973; Marsh, 1979). Further observations in Central America, however, closely linked the distribution of volcanoes to lithospheric structures. This emphasised the role of arc lithosphere in controlling magma transport (Buckart and Self, 1985; Phipps Morgan et al., 2008; Bolge et al., 2009).

Unlike Central America, the central Sunda Arc segments are not clearly linked to large crustal blocks but the observed en echelon geometry is a characteristic feature of structural systems. Analogous examples, such as mineralised tension gashes and dyke swarms, show that en echelon structures are often important fluid transport pathways. Therefore, a plausible interpretation of the central Sunda Arc is that magma is focused into volcanic systems by lithospheric scale linear structures. It may be argued that faults/fractures are rarely perfectly straight, but tectonic structural features are almost the sole cause of linear geological features on various scales. Indeed many examples of large linear faults exist and a stress-related interpretation is the most straightforward.

There are several kinematic scenarios that might generate the orientations and en echelon geometry of the central Sunda volcanic segments. Although each is considered separately in the following sections, given the complexity of the tectonics in the area it is unlikely any one scenario provides the sole causative mechanism.

5.1.1. Extension

En echelon geometries can be produced by laterally offset normal faults in which further extensional relays are developed within the zones of fault overlap (e.g. Peacock and Sanderson, 1991). There is little surface evidence for such faulting, however arc-normal extension has formed localised basins, such as the Bandung Basin and the Madura Sea (Dam et al., 1996; Kusumastuti et al., 2002). Slab rollback could cause long-term, arc-normal tension in the arc lithosphere (Macpherson and Hall, 2002) that may only intermittently become of sufficient magnitude to produce basin-scale subsidence. Alternatively, McCaffrey (1996) inferred sinistral motion of the Javan forearc from earthquake slip vectors, which could be reconciled with an extensional arc if the forearc was rotating anticlockwise with respect to Eurasia. The Roo Rise is currently being subducted beneath east Java, potentially obstructing subduction there and providing an opportunity for more effective slab rollback, and thus arc tension, further to the west (Fig. 2).

5.1.2. Strike-slip or oblique tectonics

Oblique convergence has been proposed for the central Sunda Arc (McCaffrey, 1996; Simon et al., 2007) and has the potential to produce large scale, en echelon features, which might focus magma into volcanic systems. This part of the arc lacks obvious morphological features or the seismicity that might be expected in such systems. However, the absence of well-developed examples of these features may reflect a weakly-developed or incipient system, therefore we briefly outline transtensional and oblique tectonic scenarios consistent with the observed segmentation.

En echelon secondary structures are well-known within strike-slip shear zones (Woodcock and Schubert, 1994). Assuming such a zone had boundaries sub-parallel to the primary tectonic features, i.e. plate margin, the segments could represent synthetic Riedel (R) shears in a dextral simple shear zone (cf. Fig. 9a and b) or a dextral transtensional system (Fig. 9c). Either scenario would require an upper plate stress field with the principle compression direction orientated oblique to the convergence vector between the Indo-Australian and Eurasian Plates (cf. Fig. 2), which could result from slab rollback and/or forearc rotation. However, geodetic data (Fig. 9a) and far field stress indicators (Tingay et al., 2010) may be more consistent with contraction or transpression across the arc (Fig. 9d). If this were the case then the en echelon segments could represent arc-parallel shear zones created by deformation partitioning along the axis of a sinistral deformation zone, analogous to the situation in Sumatra (McCaffrey, 1996).

5.1.3. Arc lithosphere flexure

In a number of subduction zones the arc lithosphere is deflected downwards because of upper mantle flow above the subducting slab (Husson, 2006). Downward flexure would induce arc-normal stress in the arc lithosphere; compressive in the shallow lithosphere and tensional towards its base (c.f. Hieronymus and Becovici, 1999). This stress field would exist along the length of the margin and so could develop and sustain coherent segments. A tensional pattern of fracture segments in the lower lithosphere could act as a means to channel magma into volcanic systems that would reproduce the segmentation at the surface. Once established, such a stress field might be reinforced by the effects of volcanic loading on the arc lithosphere (Hieronymus and Becovici, 1999).

In summary, there are several mechanisms associated with tectonics and flexure of the arc lithosphere that could contribute to the en echelon alignment of central Sunda volcanic segments. It is beyond the scope of this work to determine the relative importance of these mechanisms but a combination of more than one is entirely feasible.

5.2. Stress in the Sunda Arc lithosphere

Špičák et al. (2005) attempted to resolve earthquakes originating in the Sunda Arc lithospheric mantle. Many of the events they located in Nusa Tenggara lie in E - W oriented zones to the north of the volcanic arc and may be associated with southward thrusting of lithosphere at the Flores Thrust (Widiyantoro et al., 2011). The remaining earthquakes occurred either in WNW – ESE oriented zones in western Java, sub-parallel to our west segment, or in NE - SW oriented zones at various points along the arc (their Fig. 4). These two orientations are similar to the primary and secondary alignments we recognised west Java (Fig. 6b). Although the seismicity does not occur directly beneath the arc, we speculate that it reflects a similar overall stress regime throughout the central Sunda Arc.

To the west of our study area, the Great Sumatran Fault developed during the Cenozoic due to oblique, north-directed subduction of the Indo-Australian Plate (McCaffrey, 1996). In Sumatra, large calderas tend to occur close to, and are developed as a result of, lateral steps in the trace of the fault (Bellier and Sébrier, 1994). Stratovolcanoes erupting intermediate lavas and pyroclastic rocks are common close to well-developed segments of the fault. Sieh and Natawidjaja (2000) questioned this relationship because only 20% of the volcanoes lie within 2 km of the trace of the fault. However, this distance is considerably smaller than the diameter (or even the radius) of most volcanic centres and, therefore, must be considered too short to account for possible offsets of volcanic vents from main magma feeder zones. Furthermore, their treatment did not consider the possible complicating effect of secondary structures. Many Sumatran volcanoes lie to the southeast of the main fault along strong basement fabrics suggesting a secondary control, similar to our proposal for Java. Thus, we concur with Bellier and Sébrier (1994) and Gasparon (2005) that there is a strong relationship between the location of volcanoes and faulting in Sumatra.

To the east of our study area the margin becomes more complex where Australian continental lithosphere has collided with the arc (Fig. 1; Harris et al., 2009; Rigg and Hall, 2011). The islands there are constructed mainly of

Neogene to Quaternary volcanic products limiting opportunities to determine basement structures by direct observation. However, there is some evidence of a lithospheric control. First, early Quaternary, now extinct, volcanoes in the Pantar Strait (immediately west of Alor, Fig. 1) appear to have exploited NE – SW basement faulting (Elburg et al., 2002). Second, although there are no long, strong alignments (such as those identified in central Sunda), the shape of eastern Flores, Lomblen and Pantar islands and the volcanic centres of eastern Flores display a diffuse ENE – WSW en echelon, almost sigmoidal, alignment, sub-parallel to the Pantar Strait. The complex pattern of volcano distribution may reflect the stress field induced when the, possibly embayed, leading edge of Australian continental crust collided with the arc (Fig. 1).

5.3. Depth to Slab

Depths from arc volcanoes to the Wadati-Benioff Zone have been used to investigate the thermal structure and melting mechanisms in subduction zones (Syracuse and Abers, 2006; England and Katz, 2010). A subducted slab and dynamic mantle wedge is the zero-order requirement to generate the petrographic and geochemical characteristics of arc magmatism. However, volcano distributions throughout the Sunda Arc, like linear volcanic segments in several other arcs (Stoiber and Carr, 1973; Marsh, 1979; Ranneft, 1979; Hughes et al., 1980), are more plausibly explained by stress in the arc lithosphere than by processes operating either within the mantle wedge or close to its interface with the slab.

In the central Sunda Arc, west segment volcanoes have an average “depth to slab” (H) value of 91 ± 7 km while the average for the east central segment is 165 ± 8 km (Fig. 8). This brackets most of the range of average H values for arcs worldwide (c.f. England and Katz, 2010). A systematic variation along the west central segment also covers much of the global *H* range but the variation is in the opposite sense to that expected for a gradual transition between the average values of the west segment and east central segment *i.e*. *H* increases towards the west, not towards the east (Fig. 8).

Convergence rate and slab dip both vary systematically along the central Sunda Arc but by less than 10% (Section 2) and in opposing senses to one another, meaning their product varies by an even smaller amount (~5%). These parameters, therefore, cannot be related to either the sense or magnitude of *H* variation along the Sunda Arc. For other locations where *H* varies significantly within individual arcs but slab geometry does not, Syracuse and Abers (2006) proposed that structures in the upper plate or thermal heterogeneity of the mantle wedge might provide local influences upon *H*. Such structures should, therefore, be a target for future exploration in the Sunda Arc. If, however, as we have inferred, the arc lithosphere exerts the primary control on volcano location then values of *H* may have less relevance for the locus of melting than previously believed. Instead, the value of *H* for any particular volcano may depend on the combination of the orientation of stresses in the arc lithosphere with the strike direction of the slab. Closer investigation of *H* variation and segmentation within other arcs is required to resolve this issue.

6. Summary

Volcanoes of the central Sunda Arc, from Java to central Flores, occur in four, en echelon, linear segments each of 500 – 750km length. These are most likely to reflect stress-controlled weakness of arc lithosphere resulting from tectonic forces generated close to the plate margin and/or arc lithosphere flexure. Deviations from the en echelon pattern in Java occur where other structures in the arc lithospheric allow magma transport. The segmentation identified in this study explains why approaches employing depth to slab have struggled to incorporate the central Sunda Arc.

East of central Flores, where Australian continental crust has been thrust beneath the fore arc, and west of the Sunda Strait, where highly oblique convergence has produced the Great Sumatran Fault, the stress regimes in the overriding plate change and volcano distributions diverge from the pattern of en echelon, linear segments in the central Sunda Arc. This empirical observation, in itself, points to an upper plate control on distribution of volcanoes throughout the Sunda Arc.

Acknowledgements

AP is grateful for the assistance of Michael McKimm (Geological Society of London) in obtaining geological maps. CGM acknowledges a period of research leave from Durham University, during which time this study was conceived. The SE Asia Research Group at University of London is thanked for funding work to understand volcanism in Java. Discussions with Robert Hall and Jeroen van Hunen were particularly helpful in developing these ideas. The editor and two anonymous reviewers are thanked for constructive comments that helped refine this contribution.

References

Audley-Charles, M.G., 2004. Ocean trench blocked and obliterated by Banda forearc collision with Australian proximal continental slope. Tectonophysics 389, 65-79.

Becker, J.J., Sandwell, D.T., Smith, W.H.F., Braud, J., Binder, B., Depner, J., Fabre, D., Factor, J., Ingalls, S., Kim, S.H., Ladner, R., Marks, K., Nelson, S., Pharaoh, A., Sharman, G., Trimmer, R., von Rosenburg, J., Wallace, G., Weatherall, P., 2009. Global Bathymetry and Elevation Data at 30 Arc Seconds Resolution: SRTM30_PLUS. Marine Geodesy 32, 355-371.

Barber, A.J., Crow, M.J., de Smet, M.J.M., 2005. Chapter 14: Tectonic evolution. In: Barber, A.J., Crow, M.J., Milsom, J.S. (Eds.), Sumatra: Geology, Resources and Tectonic Evolution, vol. 31. Geological Society, London Memoirs, pp. 234-259.

Bellier, O., Sébrier, M., 1994. Relationship between tectonism and volcanism along the Great Sumatran Fault Zone deduced by SPOT image analyses. Tectonophysics 233, 215-231.

Bolge, L.L., Carr, M.J., Milidakis, K.I., Lindsay, F.N., Feignenson, M.D., 2009. Correlating geochemistry, tectonics, and volcanic volume along the Central volcanic front. Geochemistry, Geophysics, Geosystems 10, Q12S18. doi:10.1029/2009GC002704.

Bouilhol, P., Schaltegger, U., Chiarardia, M., Ovtcharova, M., Stracke, A., Burg, J.-P., Dawood, H., 2010. Timing of juvenile arc crust formation and evolution in the Sapat Complex (Kohistan-Pakistan). Chemical Geology 280, 243-256.

Buckart, B., Self, S., 1985. Extension and rotation of crustal blocks in northern Central America and effect on the volcanic arc. Geology 13, 22-26.

Carr, M.J., Stoiber, R.E., Drake, C.L., 1973. Discontinuities in the deep seismic zone under the Japanese arcs. Bull. Geol. Soc. Am. 84, 2917-2930.

Carranza, E.J.M., Wibowo, H., Barritt, S.D., Sumintadireja, P., 2008. Spatial data analysis and integration for regional-scale geothermal potential mapping, West Java, Indonesia. Geothermics 37, 267-299.

Clements, B., Hall, R., Smyth, H.R., Cottam, M.A., 2009. Thrusting of a volcanic arc: a new structural model for Java. Petroleum Geoscience 15, 159-174.

Connor, C.B., 1990. Cinder cone clustering in the TransMexican Volcanic belt: Implications for structural and petrological models. Journal of Geophysical Research 95, 19395-19405.

Connor, C.B., Condit, C.D., Crumpler, L.S., Aubele, J.C., 1992. Evidence of regional structural control on vent distribution: Springerville Volcanic Field, Arizona. Journal of Geophysical Research 97, 12349-12359.

Cooper, G.R.J., 2006a. Geophysical applications of the Hough Transform. South African Journal of Geology 109, 555-560.

Cooper, G.R.J., 2006b. Obtaining dip and susceptibility information from Euler decovolution using the Hough Transform. Computers and Geoscience 32, 1592-1599.

Dam, M.A.C., Suparan, P., Nossin, J.J., Voskuil, R.P.G.A., GTL Group, 1996. A chronology for geomorphological developments in the greater Bandung area, West-Java, Indonesia. Journal of Southeast Asia Earth Sciences 14, 101-115.

Dempsey, S.R. 2013. Geochemistry of volcanic rocks from the Sunda Arc. PhD thesis, Durham University.

Dunda, R.O., Hart, P.E., 1971, Use of the Hough Transformation to detect lines and curves in pictures. Communications of the ACM 15, 11-15.

Edwards, C., Menzies, M., Thirlwall, M., 1991. Evidence from Muriah, Indonesia, for the interplay of supra-subduction zone and intraplate processes in the genesis of potassic alkaline magmas. Journal of Petrology 32, 555-592.

Edwards, C.M.H., Menzies, M.A., Thirlwall, M.F., Morris, J.D., Leeman, W.P., Harmon, R.S., 1994. The Transition to Potassic Alkaline Volcanism in Island Arcs: The Ringgit—Beser Complex, East Java, Indonesia. Journal of Petrology 35, 1557-1595.

Elburg, M.A., van Bergen, M., Hoogewerff, J., Foden, J., Vroon, P., Zulkarnain, I., Nasution, A., 2002. Geochemical trends across an arc-continent collision zone: magma sources and slab-wedge transfer processes below the Pantar Strait volcanoes, Indonesia. Geochimica et Cosmochimica Acta 66, 2771-2789.

England, P.C., Katz, R.F., 2010. Melting above the anhydrous solidus controls the location of volcanic arcs. Nature 467, 700-703.

England, P., Engdahl, R., Thatcher, W., 2004. Systematic variations in the depth of slabs beneath arc volcanoes. Geophysical Journal International 156, 377-408.

Fischler, M.A., Bolles, R.C., 1981. Random sample consensus: a paradigm for model fitting with applications to image analysis and automated cartography. Communications of the ACM 24, 381-395.

Foden, J., 1986. The petrology of Tambora volcano, Indonesia: A model for the 1815 eruption. Journal of Volcanology and Geothermal Research 27, 1-41.

Foden, J.D., Varne, R., 1980. The petrology and tectonic setting of Quaternary - Recent volcanic centres of Lombok and Sumbawa, Sunda arc. Chemical Geology 30, 201-226.

Gasparon, M., 2005. Chapter 9: Quaternary volcanicity. In: Barber, A.J., Crow, M.J., Milsom, J.S. (Eds.), Sumatra: Geology, Resources and Tectonic Evolution, vol. 31. Geological Society London Memoirs, pp. 120-130.

Granath, J.W., Christ, J.M., Emmet, P.A., Dinkelman, M.G., 2011. Pre-Cenozoic sedimentary section and structure as reflected in the JavaSPAN™ crustal-scale PSDM seismic survey, and its implications regarding the basement terranes in the East Java Sea. In: Hall, R., Cottam, M.A., Wilson, M.E.J. (Eds.), The SE Asian Gateway: History and Tectonics of the Australia-Asia Collision vol. 355. Geological Society London Special Publications, pp. 53-74.

Grove, T.L., Till, C.B., Lev, E., Chatterjee, N., Médard, E., 2009. Kinematic variables and water transport control the formation and location of arc volcanoes. Nature 459, 694-697.

Hall, R., 2011. Australia-SE Asia collision: plate tectonics and crustal flow. In: Hall, R., Cottam, M.A., Wilson, M.E.J. (Eds.), The SE Asian Gateway:

History and Tectonics of the Australia-Asia Collision vol. 355. Geological Society London Special Publications, pp. 75-109.

Hall, R., 2012. Later Jurassic – Cenozoic reconstructions of the Indonesian region and the Indian Ocean. Tectonophysics 570, 1-41

Harris, R., Vorkin, M.W., Prasetyadi, C., Zobell, E., Roosmawati, N., Apthorpe, M., 2009. Transition from subduction to arc-continent collision: Geologic and neotectonic evolution of Savu Island, Indonesia. Geosphere 5, 152-171.

Hart, P.E., 2009. How the Hough Transform was Invented. IEEE Signal Processing Magazine 26, 18-22.

Hieronymus, C., Bercovici, D., 1999. Discrete alternating hotspot islands formed by interaction of magma transport and lithospheric flexure. Nature 397, 604-607.

Hughes, J.M., Stoiber, R.E., Carr, M.J., 1980. Segmentation of the Cascade volcanic chain. Geology 8, 15-17.

Husson, L., 2006. Dynamic topography above retreating subduction zones. Geology 34, 741-744.

Jarvis, A., Reuter, H.I., Nelson, A., Guevara, E., 2008. Hole-filled seamless SRTM data v4. International Centre for Tropical Agriculture (CIAT), http://srtm.csi.cgiar.org.

Jenkins, C., Wan, J., Holden, E.-J., Dentith, M., Kovesi, P.D., Haederle, M., 2008. Application of Radial Symmetry for Caldera Detection, Digital Image Computing: Techniques and Applications DICTA 2008, vol. 1. Los Alamitos, California, USA, pp. 142-147.

Karnieli, A., Meisels, A., Fisher, L., Arkin, Y., 1996. Automatic extraction and evaluation of geological linear features from digital remote sensing data using a Hough Transform. Photogrammetric Engineering & Remote Sensing 62, 525-531.

Kusumastuti, A., Van Rensbergen, P., Warren, J.K., 2002. Seismic sequence analysis and reservoir potential of drowned Miocene carbonate platforms in Madura Strait, east Java, Indonesia. AAPG Bulletin 86, 213-232.

Leterrier, J., Yuwono, Y.S., Soeria-Atmadja, R., Maury, R.C., 1990. Potassic volcanism in Central Java and South Sulawesi, Indonesia. Journal of Southeast Asian Earth Sciences 4, 171-187.

Lunt, P., Burgon, G., Baky, A., 2009. The Pemali Formation of central Java and equivalents: Indicators of sedimentation on an active plate margin. Journal of Asian Earth Sciences 34, 100-113.

Macpherson C.G., 1994. New analytical approaches to the oxygen and carbon stable isotope geochemistry of some subduction-related lavas. PhD thesis, University of London.

Macpherson, C.G., Hall, R., 2002. Timing and tectonic controls in the evolving orogen of SE Asia and the western Pacific and some implications for ore generation. In: Blundell, D.J., Neubauer, F., von Quant, A. (Eds.), The Timing and Location of Major Ore Deposits in an Evolving Orogen, vol. 204. Geological Society London Special Publications, 49-67.

Marsh, B.D., 1979. Island arc development: Some observations, experiments, and speculations. Journal of Geology 87, 687-713.

McCaffrey, R., 1996. Slip partitioning at convergent plate boundaries of SE Asia. In: Hall, R., Blundell, D. (Eds.), Tectonic Evolution of SE Asia, vol. 106. Geological Society London Special Publications, pp. 3-18.

Peacock, D.C.P., Sanderson, D.J., 1991. Displacements, segment linkage and relay ramps in normal fault zones. Journal of Structural Geology, 13, 721-733.

Phipps Morgan, J., Ranero, C.R., Vannucchi, P., 2008. Intra-arc extension in Central America: links between plate motions, tectonics, volcanism, and geochemistry. Earth and Planetary Science Letters 272, 365-371.

Pringgoprawiro, H., Sukido, 1992. Geological map of the Bojonegoro Quadrangle, East Java (1:100,000) sheet 1508-5. Geological Research and Development Centre, Bandung.

Ranneft, T.S.M., 1979. Segmentation of island arcs and application to petroleum geology. Journal of Petroleum Geology 1, 35-53.

Rigg, J.W.D., Hall, R., 2011. Structural and stratigraphic evolution of the Savu Basin, Indonesia. In: Hall, R., Cottam, M.A., Wilson, M.E.J. (Eds.), The SE Asian Gateway: History and Tectonics of the Australia-Asia Collision vol. 355. Geological Society London Special Publications, pp. 225-240.

Rivera, S.L., Pardo, R., 2004. Discovery and geology of the Toki porphyry copper deposit, Chuquicamata district, northern Chile. Society of Economic Geologists Special Publication 11, 199−211.

Sæther, B., Rueslatten, H., Grøenlie, A., 1994. Application of the Hough Transform for automated interpretation of linear features in imageries, vol. 2. Geoscience and Remote Sensing Symposium 1994, pp. 847-850.

Sanderson, D.J., Marchini, W.R.D., 1984, Transpression: Journal of Structural Geology 6, 449-458.

Siebert, L., Simkin, T., 2002. Volcanoes of the world: An illustrated catalogue of Holocene volcanoes and their eruptions. Global Volcanism Program Digital Information Service, GVP-3. Smithsonian Institute, Washington, D.C. (Available at http://www.volcano.si.edu/world)

Sieh, K., Natawidjaja, D., 2000. Neotectonics of the Sumatran fault, Indonesia. Journal of Geophysical Research 105, 28,295-28,326.

Simons, W.J.F., Socquet, A., Vigny, C., Ambrosius, B.A.C., Haji Abu, S., Promthong, C., Subarya, C., Sarsito, D.A., Matheussen, S., Morgan, P., Spakman, W., 2007. A decade of GPS in Southeast Asia: Resolving Sundaland motion and boundaries. Journal of Geophysical Research 112, B06420.

Smyth, H.R., Hamilton, P.J., Hall, R., Kinny, P.D., 2007. The deep crust beneath island arcs: Inherited zircons reveal a Gondwana continental fragment beneath East Java, Indonesia. Earth and Planetary Science Letters 258, 269-282.

Socquet, A., Vigny, C., Chamot-Rooke, N., Simons, W., Rangin, C., Ambrosius, B., 2006. India and Sunda plates motion and deformation along their boundary in Myanmar determined by GPS: Journal of Geophysical Research 111, B05406.

Spakman, W., Hall, R., 2010. Surface deformation and slab-mantle interaction during Banda arc subduction rollback. Nature Geoscience 3, 562-566.

Špičák, A., Hanuš, V, Vaněk, J., 2005. Seismotectonic pattern and the source region of volcanism in the central part of the Sunda Arc. Journal of Asian Earth Sciences 25, 583-600.

Stoiber, R.E., Carr, M.J., 1973. Quaternary volcanic and tectonic segmentation of Central America. Bulletin Volcanologique 37, 326-337.

Syracuse, E.M., Abers, G.A., 2006. Global compilation of variations in slab depth beneath arc volcanoes and implications. Geochemistry, Geophysics, Geosystems 7, Q05017. doi:10.1029/2005GC001045.

Tikoff, B., Teyssier, C., 1992. Crustal-scale, en echelon “P-shear” tensional bridges: A possible solution to the batholithic room problem. Geology 20, 927-930.

Tingay, M., Morley, C., King, R., Hillis, R., Coblentz, D., Hall, R., 2010. Present-day stress field in Southeast Asia. Tectonophysics, 482, 92-104.

Tosdal, R.M., Richards, J.P., 2001. Magmatic and structural controls on the development of porphyry Cu ± Mo ± Au deposits. In: Richards, J.P., Tosdal, R.M. (Eds.), Reviews in Economic Geology 14, 157-181.

Wadge, G., Cross, A., 1988. Quantitative methods for detecting aligned points: An application to the volcanic vents of the Michoacan-Guanajuato volcanic field, Mexico. Geology 16, 815-818.

Wang, J., Howarth, P.J., 1990. Use of the Hough transform in automated lineament detection. IEEE Transactions on Geoscience and Remote Sensing 28, 561-566

Whitford, D.J., 1975. Strontium isotopic studies of the volcanic rocks of the Sunda arc, Indonesia, and their petrogenetic implications. Geochimica et Cosmochimica Acta 39, 1287-1302.

Widiyantoro, S., Pesicek, J.D., Thurber, C.H., 2011. Subducting slab structure below the eastern Sunda arc inferred from non-linear seismic tomographic imaging. In: Hall, R., Cottam, M.A., Wilson, M.E.J. (Eds.), The SE Asian Gateway: History and Tectonics of the Australia-Asia Collision vol. 355. Geological Society London Special Publications, pp. 139-155.

Woodcock, N.H., Schubert, C. 1994. Continental strike-slip tectonics. In: Hancock, P.L. (Ed.), Continental Deformation, Pergamon Press, New York, pp. 251-236.

Yamaji, A., Otsubo, M., Sato, K., 2006. Paleostress analysis using the Hough transform for separating stress from heterogeneous fault-slip data. Journal of Structural Geology 28, 980-990.

Zaliapin, I., Gabrielov, A., Keilis-Borok, V., 2004. Multiscale Trend Analysis. Fractals 12, 275-292.

Figure Captions

Figure 1. Map of Indonesia showing the major islands and tectonic structures, modified from Macpherson and Hall (2002). Active subduction zones are thick lines with barbs on the overriding plate. Other solid lines represent inactive subduction zones or major strike-slip faults; GSF: Great Sumatran Fault. Black dotted line represents the estimated northern extent of Australian continental crust subducted at the Timor Trough (Harris et al., 2009). Grey dashed lines represent the estimated accretion ages of Gondwanan lithospheric terranes to Sundaland (Hall, 2011).

Figure 2. Relief of the central Sunda Arc produced from topographic (SRTM v.4) and bathymetric (SRTM30 Plus v.7 of Becker et al., 2009) base datasets. Black arrows showing convergence directions of the Indo-Australian Plate and Sundaland are labelled with convergence rates (Simons et al., 2007). Triangles represent all geologically validated Quaternary volcanic structures with a basal diameter >3 km. Seafloor colour coded for depth (cooler colours for greater depth). Volcanoes labelled are: Arjuno-Welirang (AW), Baluran (Bl), Batur (Bt), Galunggung (Gg), Kawi-Butak (KB), Krakatau (Kr), Lasem (La), Merapi (Me), Muriah (Mu), Papandan (Pa), Ringgit-Beser (Ri), Sangeang Api (SA), Sangenges (Sa), Semeru (Se), Slamet (Sl), Sumbing (Su), Tambora (Ta), Tankuban Prahu (TP), Tengger Caldera (TC) and Wilis (Wi). Yellow triangles represent centres omitted from outset due to petrological and/or geochronological differences to arc volcanics (see text for details).

Figure 3. Schematic illustration showing application of Hough Transform analysis to recognise alignment. Lines with all possible azimuths are passed through each point in a dataset. Grey lines in panels (a) and (b) illustrate two

such lines each for the square and the triangle, respectively. For lines of all azimuths the normal that passes through the origin (dashed lines) is identified and the length (ρ) and angle to the x-axis (θ) are plotted against one another (parameter space plot) giving a sinusoidal trace for each point. This is illustrated in panel (c), where the open symbols are the examples shown in panels (a) and (b) and closed symbols represent normals to lines with other azimuths (omitted from (a) and (b) for clarity). Aligned points return the same coupled ρ – θ values (e.g. normals 1 and 4). Therefore, increased frequency of such pairs (effectively a third axis projecting out of the page) is a means of identifying alignments in datasets.

Figure 4. Hough Transform analysis of the (a) uniform, and (b) weighted volcanic datasets for the central Sunda Arc. All images are proportionate i.e. horizontal scale = vertical scale. Volcanic structures are represented by (a) filled circles of uniform size, and (b) circles three-quarters the measured basal diameter of the structure. Straight lines are the alignments identified by Hough Transform analysis. Varying shades and ornaments are used simply to aid distinction of potential alignments. (c) Alignments that occur in both the uniform and weighted datasets (labelled with R^2 values) for all circles that fall within the associated ellipses. (d) Four alignments (and R^2 values) identified by forcing circles to only lie in one alignment.

Figure 5. Plot of K_2O versus MgO for volcanic rocks from Java. Backarc volcanoes (Leterrier et al., 1990; Edwards et al., 1991; Edwards et al., 1994; Macpherson, 1994), plotted as discrete symbols, are significantly more potassic than the volcanic arc (Dempsey, 2013).

Figure 6. SRTM data for Java and Bali summarising significant structures from 1:100,000 scale geological mapping (Supplementary Material A). Triangles are volcanic centres included in the initial Hough Transform analysis (Fig. 4). Orange centres trend away from the segments identified in Fig. 4 but are aligned sub-parallel to other local structures. (b) Enlarged view of the Bandung area (white box in panel a) illustrating the distinct structural 'grains' which are approximated by the two black lines shown; the longer line is sub-parallel to the volcanic segments identified in Fig. 4. (c) Enlarged view of the black box in panel (a) showing that Pandan lies within a Tertiary fold belt, across which folded strata are apparently offset and warped.

Figure 7. Results of linear least squares regression for the central Sunda Arc weighted dataset after excluding those centres probably related to second order lithospheric control (see text and Fig. 6). Regression lines (solid) with R^2 values and 95% confidence interval (dashed lines). For clarity, the northing scale is exaggerated relative to the easting scale.

Figure 8. Latitude versus depth to the top of the Wadati-Benioff Zone (*H*) for Java, Bali and Lombok using data from Syracuse and Abers (2006), which provides little data for volcanoes from the east segment. Symbols are based on the alignments identified in this work (Fig. 7). Squares represent volcanoes excluded from our spatial analysis on the basis of petrography, geochemistry and possible secondary influence of mesoscale lithospheric structures (Section 5).

Figure 9. (a) The central Sunda Arc in UTM projection, with coordinates referring to UTM zone 48S; arrows represent GPS-derived movement vectors from GEODYSSEA stations with respect to the Sunda Plate (Socquet et al.,

2006). Black lines show the volcanic segments identified in Fig. 7. (b) Plan view showing the orientation and sense of secondary structures in a dextral simple shear zone with respect to the principal stress axes. R and R’ are the synthetic and antithetic Riedel shears, respectively, T is tensile fracturing and P is P shearing (after Woodcock and Schubert, 1994). Zones of (c) dextral transtension, and (d) dexteral transpression in plan view showing the orientation and sense of structures with respect to the principal stress axes (Sanderson and Marchini, 1984). Strain ellipsoids also shown. Abbreviations as in (b) plus; TF - Thrust Fault, NF - Normal Fault, and F - Fold.

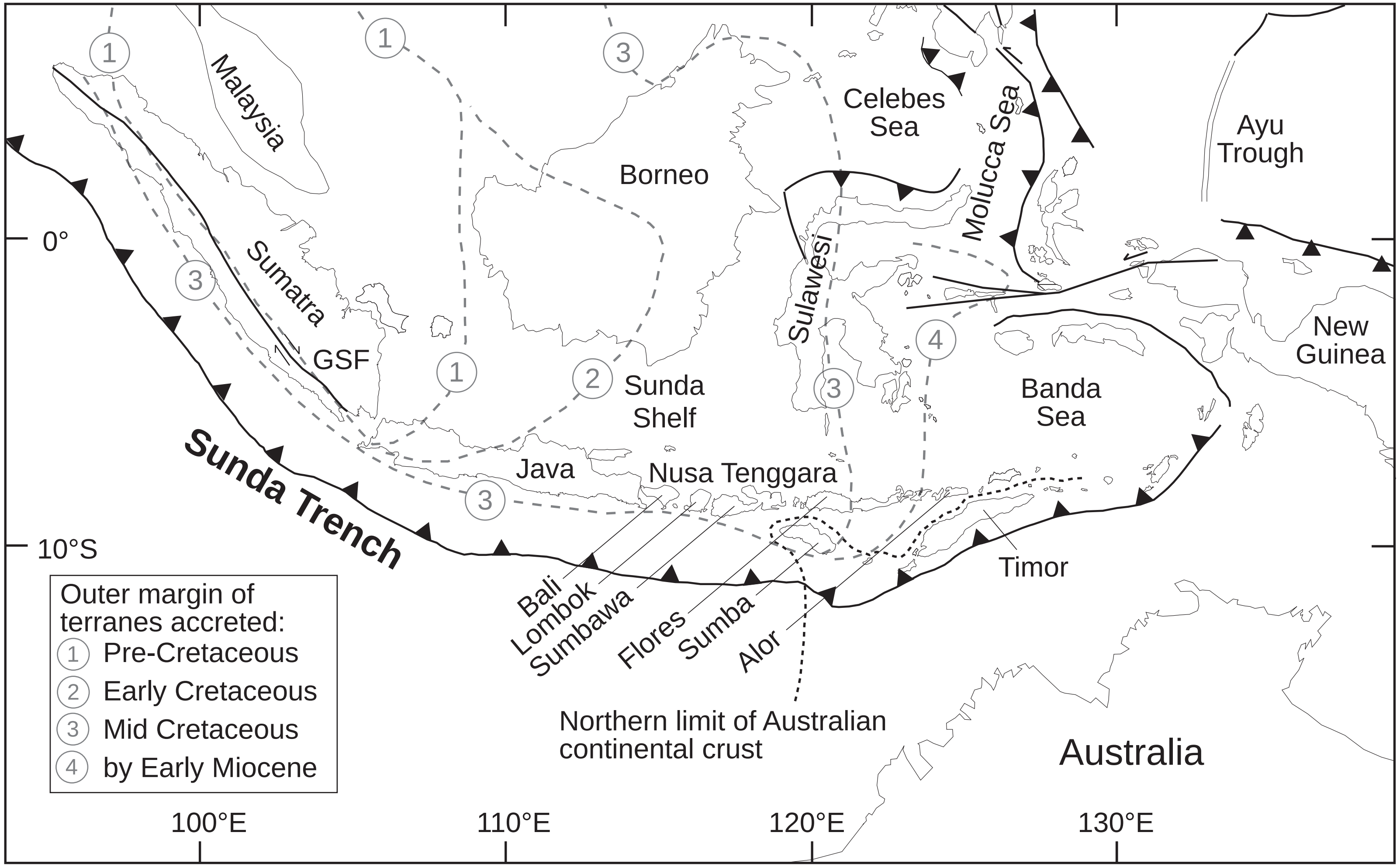
Malaysia
Sumatra
GSF
Borneo
Sunda Shelf
Java
Sunda Trench
Nusa Tenggara
Celebes Sea
Sulawesi
Molucca Sea
Ayu Trough
New Guinea
Banda Sea
Timor
Bali
Lombok
Sumbawa
Flores
Sumba
Alor
Northern limit of Australian continental crust
Australia
0°
10°S
100°E
110°E
120°E
130°E
Outer margin of terranes accreted:
1 Pre-Cretaceous
2 Early Cretaceous
3 Mid Cretaceous
4 by Early Miocene

Figure 1

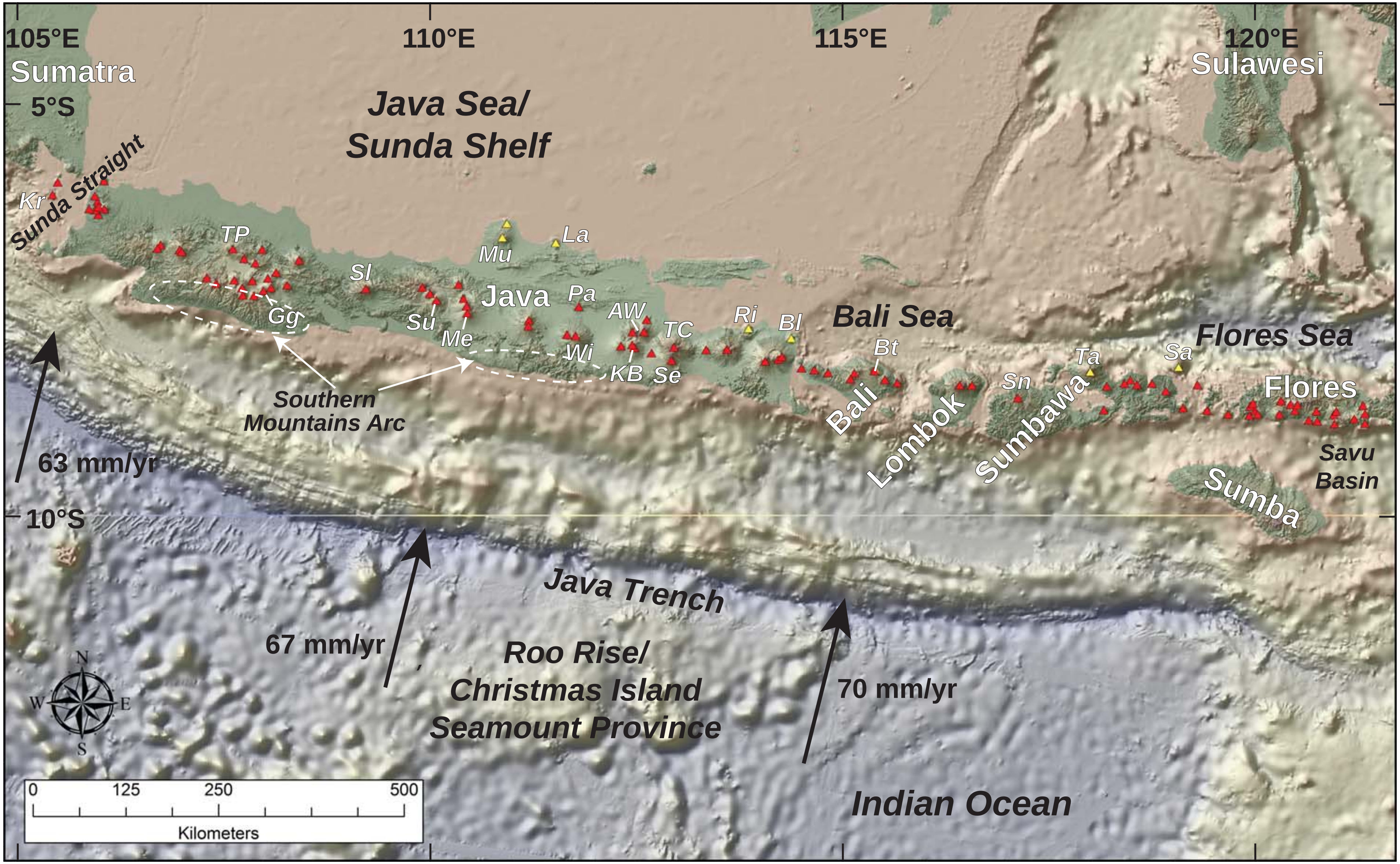
105°E
110°E
115°E
120°E
5°S
10°S
Sumatra
Sulawesi
Java Sea/
Sunda Shelf
Sunda Straight
Kr
TP
Gg
Sl
Su
Me
Mu
La
Java
Pa
Wi
AW
KB
TC
Se
Ri
Bl
Bali Sea
Bt
Bali
Lombok
Sn
Sumbawa
Ta
Sa
Flores Sea
Flores
Savu
Basin
Sumba
Southern
Mountains Arc
63 mm/yr
67 mm/yr
70 mm/yr
Java Trench
Roo Rise/
Christmas Island
Seamount Province
Indian Ocean
N
E
S
W
0
125
250
500
Kilometers

Figure 2

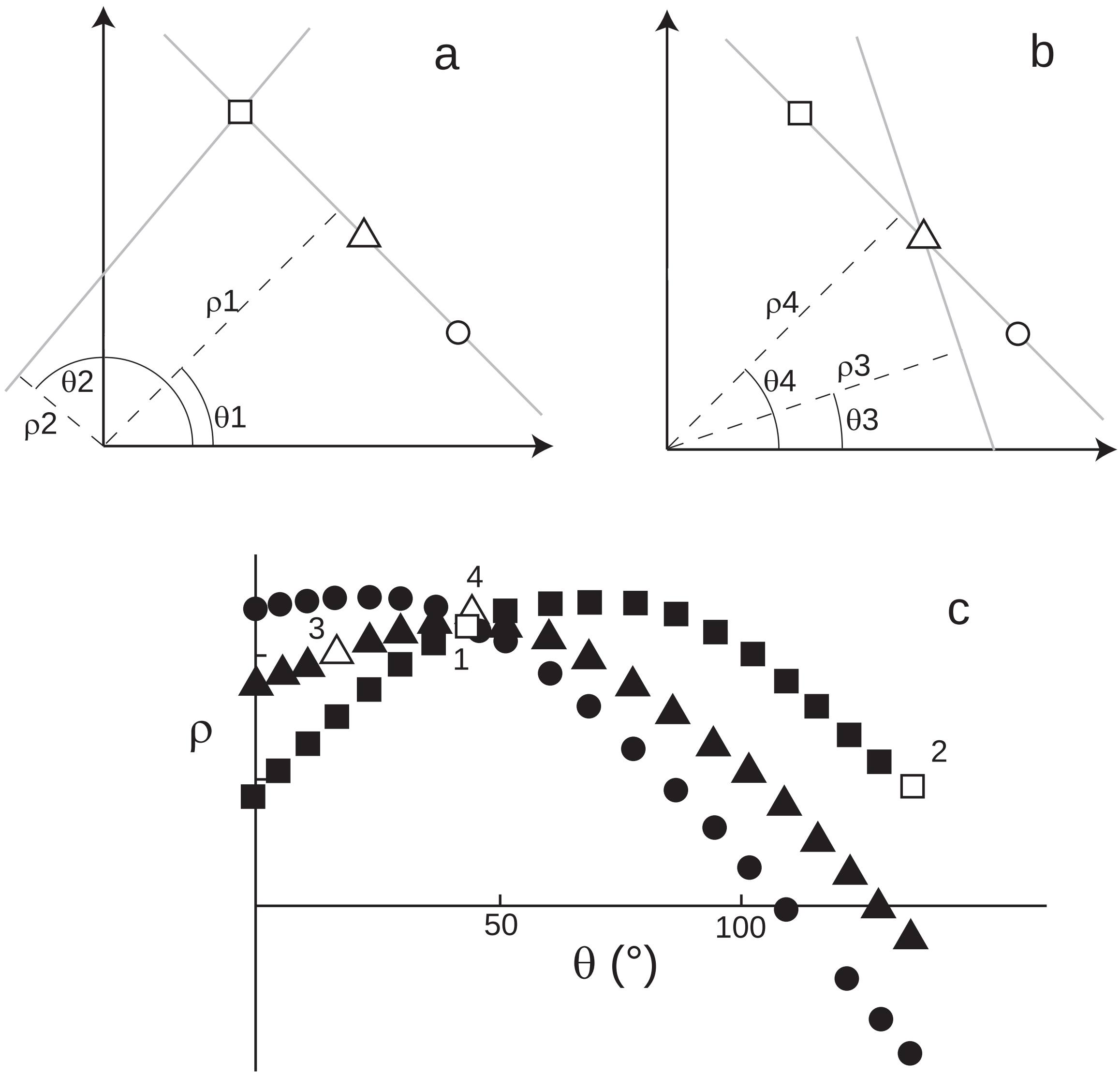

Figure 3

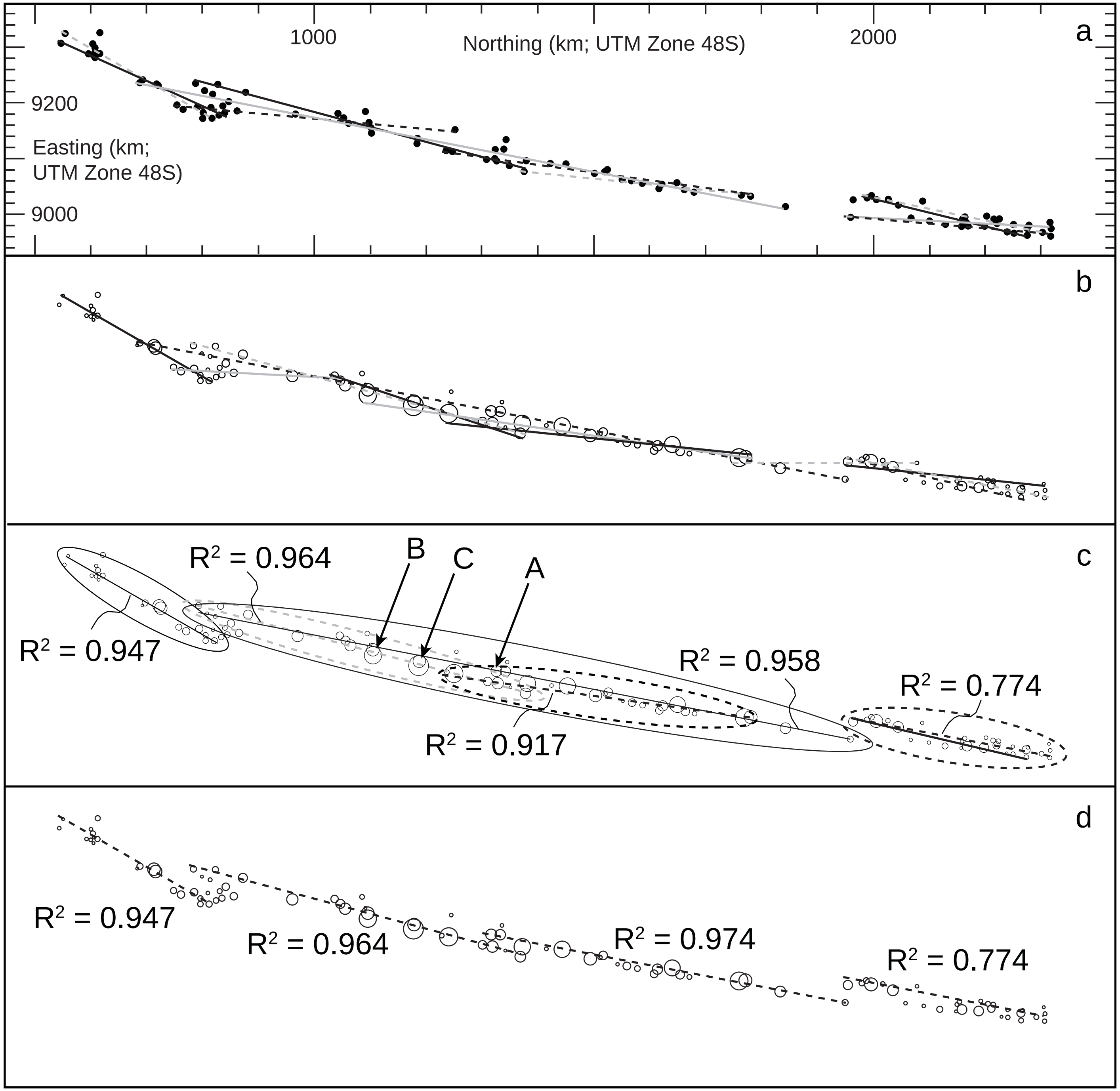
a
b
c
d
Northing (km; UTM Zone 48S)
1000
2000
Easting (km;
UTM Zone 48S)
9200
9000
R² = 0.947
R² = 0.964
B
C
A
R² = 0.958
R² = 0.917
R² = 0.774
R² = 0.947
R² = 0.964
R² = 0.974
R² = 0.774

Figure 4

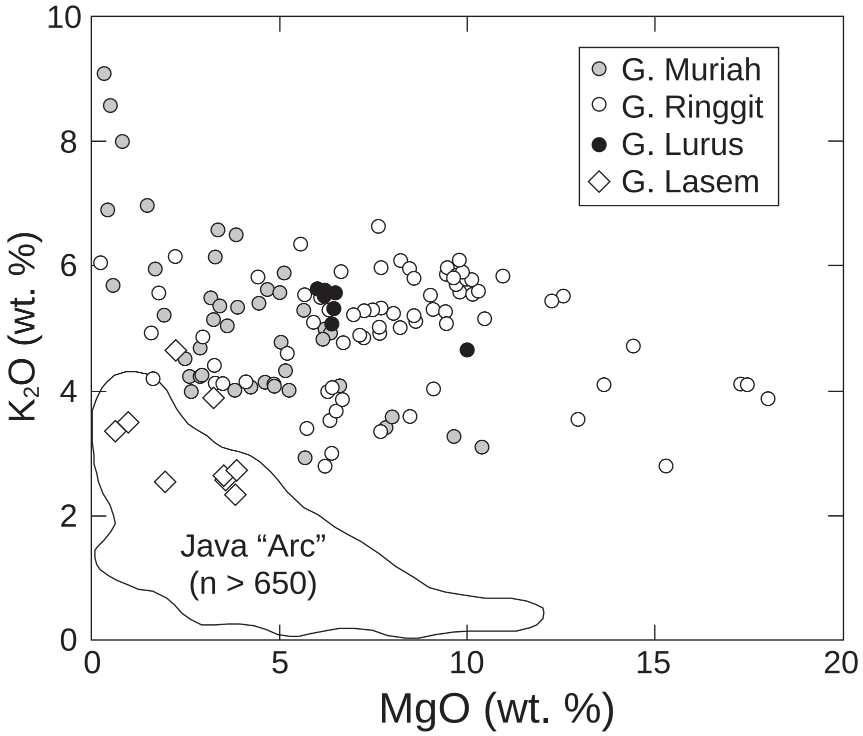
G. Muriah
G. Ringgit
G. Lurus
G. Lasem
Java "Arc"
(n > 650)
K_2O (wt. %)
MgO (wt. %)
0
2
4
6
8
10
0
5
10
15
20

Figure 5

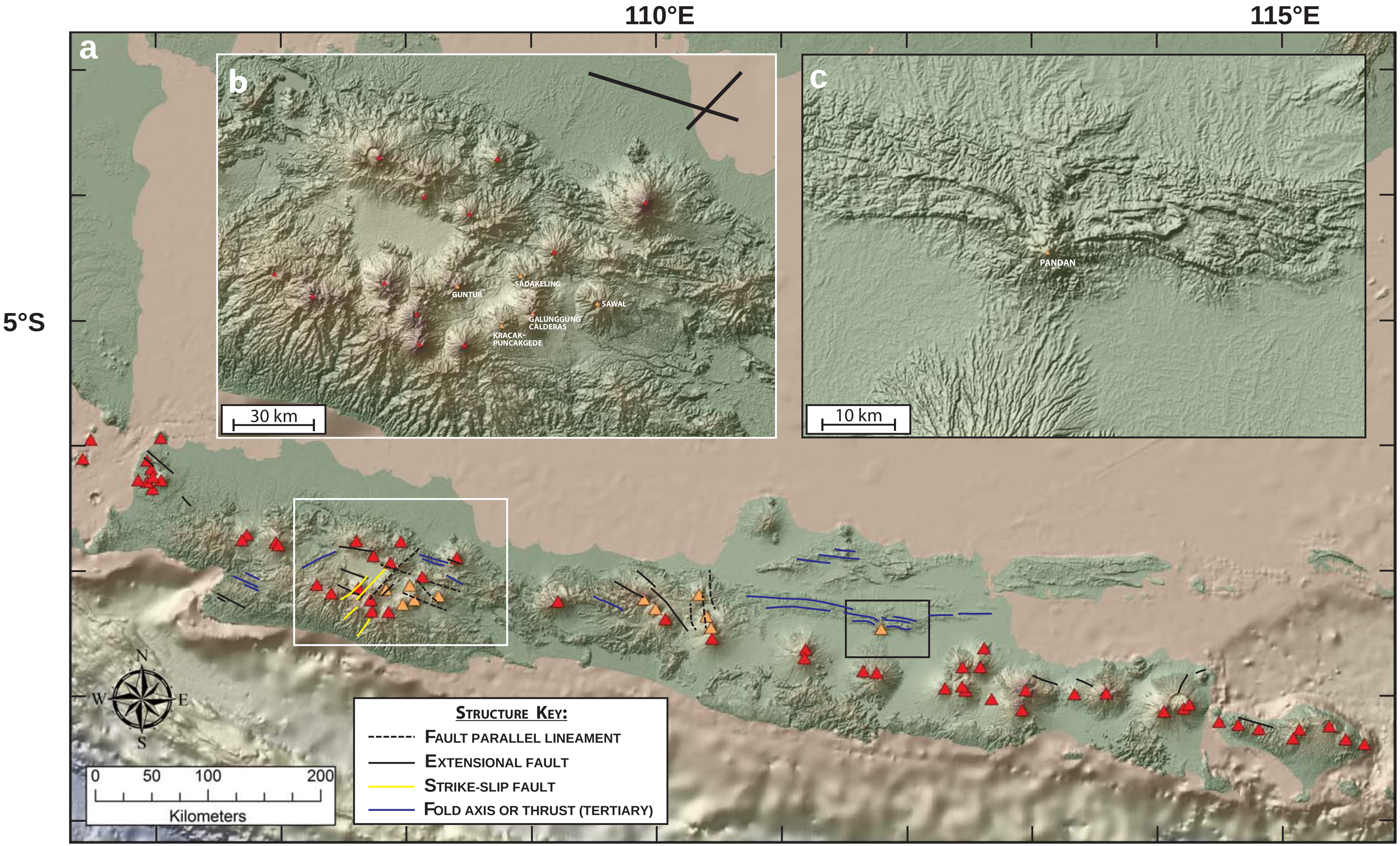
110°E
115°E
5°S
a
b
c
30 km
10 km
GUNTUR
SADAKELING
SAWAL
GALUNGGUNG CALDERAS
KRACAK-PUNCAKGEDE
PANDAN
STRUCTURE KEY:
FAULT PARALLEL LINEAMENT
EXTENSIONAL FAULT
STRIKE-SLIP FAULT
FOLD AXIS OR THRUST (TERTIARY)
0 50 100 200
Kilometers
N
E
S
W

Figure 6

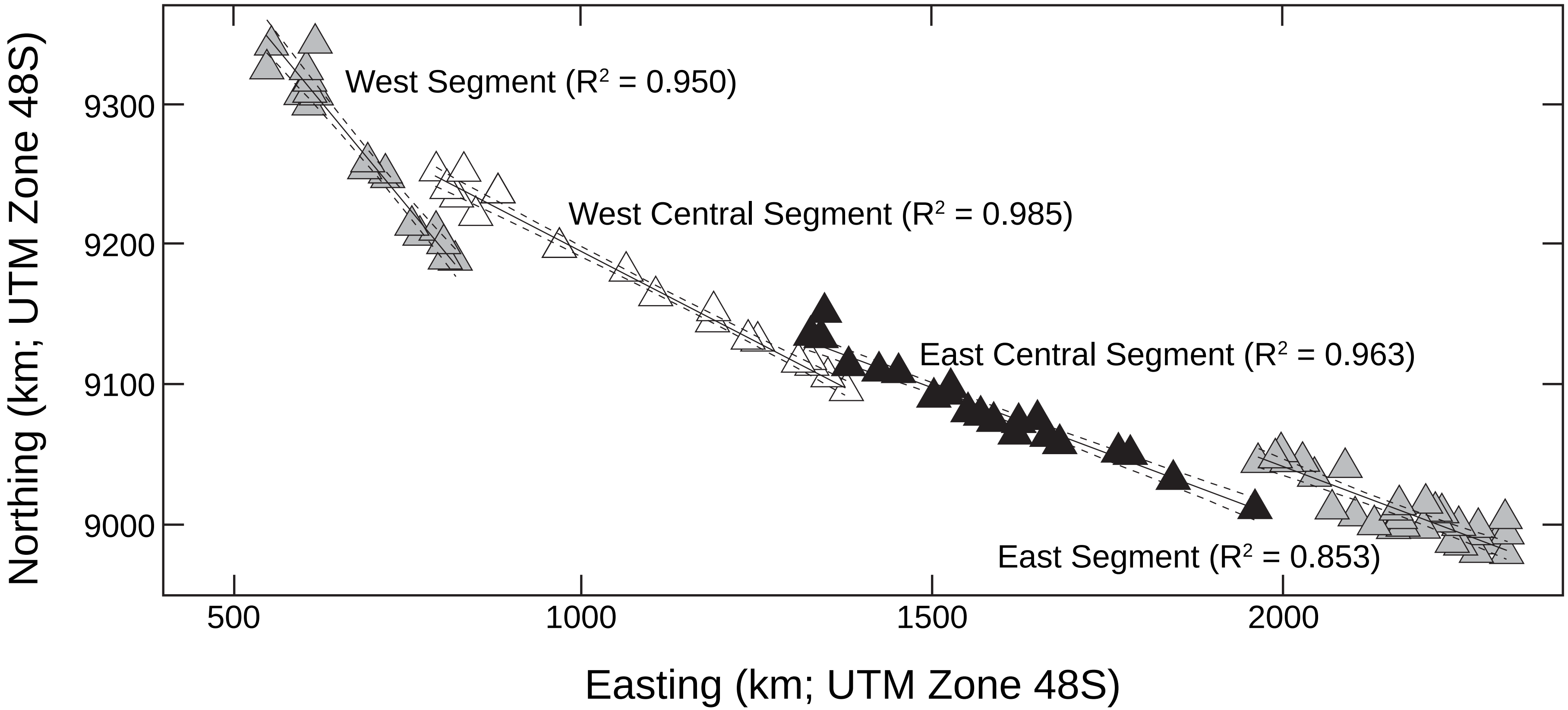

West Segment (R² = 0.950)
West Central Segment (R² = 0.985)
East Central Segment (R² = 0.963)
East Segment (R² = 0.853)
9300
9200
9100
9000
Northing (km; UTM Zone 48S)
500
1000
1500
2000
Easting (km; UTM Zone 48S)

Figure 7

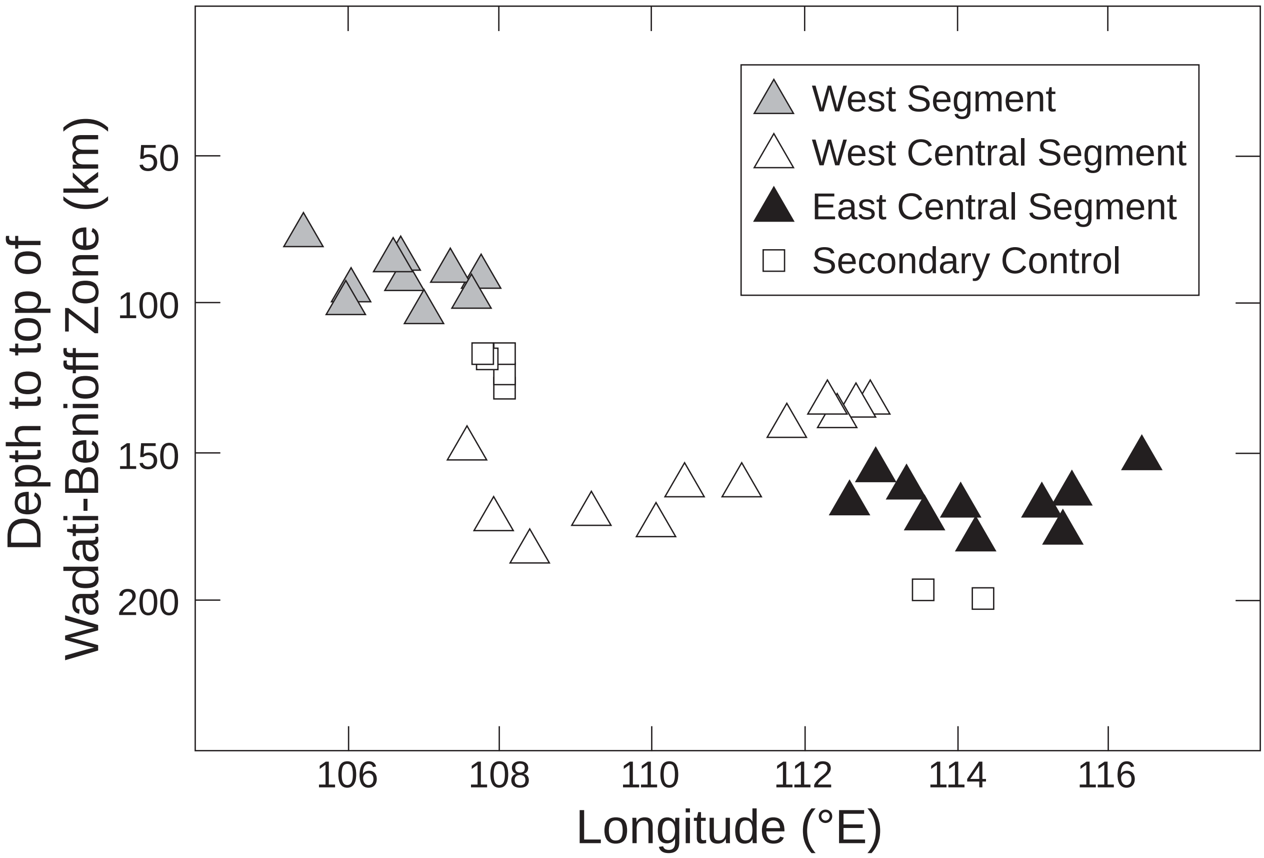
West Segment
West Central Segment
East Central Segment
Secondary Control
Depth to top of
Wadati-Benioff Zone (km)
50
100
150
200
106
108
110
112
114
116
Longitude (°E)

Figure 8

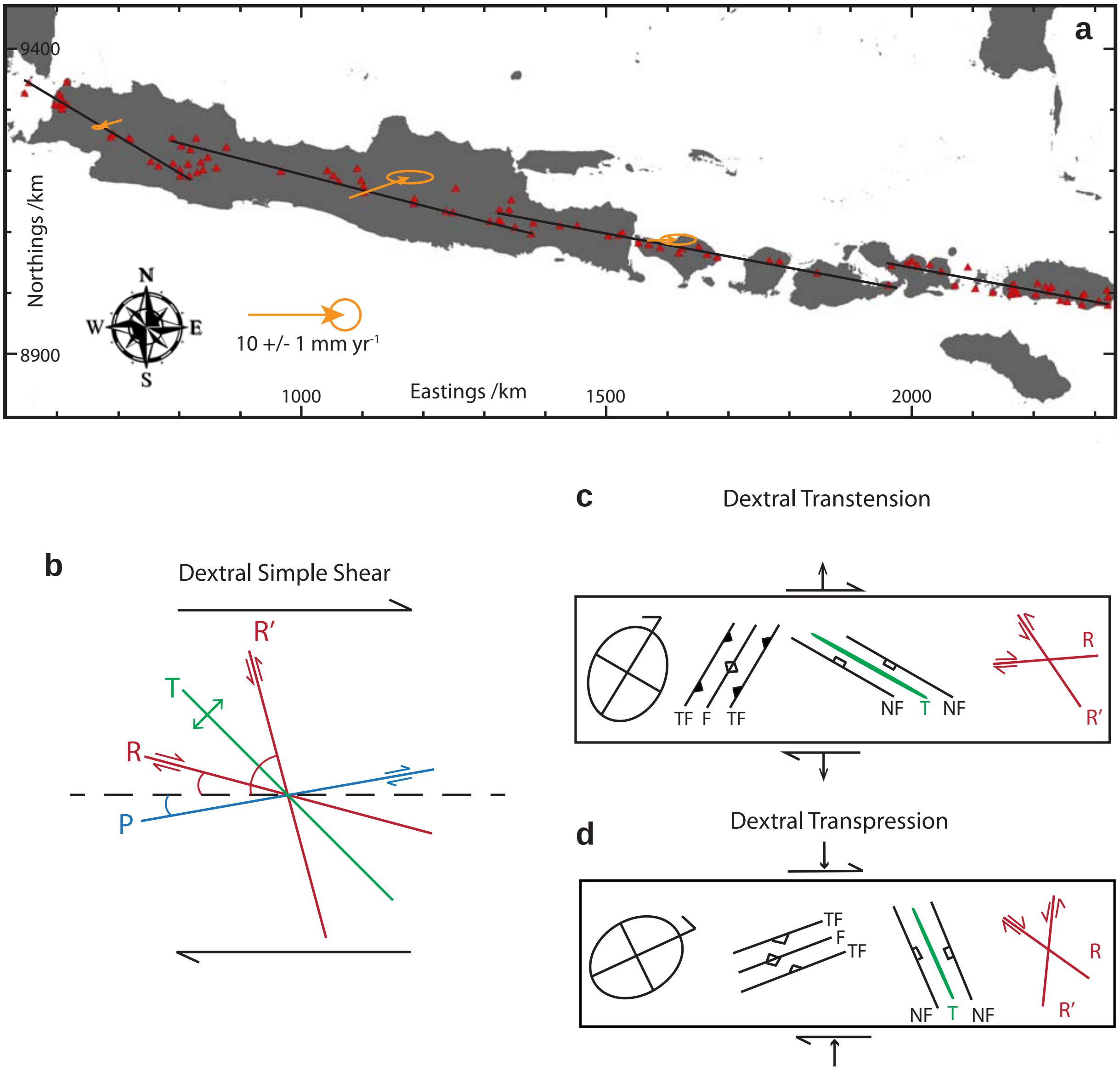

a
9400
8900
Northings /km
Eastings /km
1000
1500
2000
N
S
W
E
10 +/- 1 mm yr-1
b
Dextral Simple Shear
R′
T
R
P
c
Dextral Transtension
TF
F
TF
NF
T
NF
R
R′
d
Dextral Transpression
TF
F
TF
NF
T
NF
R
R′

Figure 9

Supplementary Material A – Indonesian Maps

Maps used to verify volcanic features in Java, Bali and Flores, all published by the Geological Research and Development Centre in Bandung, Indoneisa.

Agustiyanto DA, Santosa S, 1993. Geological map of the Situbondo Quadrangle, Java (1:100,000).

Alzwar M, Akbar N, Bachri S, 1992. Geological map of the Garut and Pameungpeuk Quadrangles, Java (1:100,000).

Andi Mangga S, Atmawinta B, Hermanto B, Setyogroho B, Amin TC, 1994. Geological map of the Lombok sheet, West Nusatenggara (1:250,000).

Condon WH, Pardyanto L, Ketner KB, Amin TC, Gafoer S, Samodra H, 1996. Geological map of the Banjarnegara and Pekalongan sheet, Java (1:100,000).

Djuri, 1995. Geological map of the Arjawinangun Quadrangle, Java (1:100,000).

Effendi AC, Kusnama, Hermanto B, 1998. Geological map of the Bogor Quadrangle, Java (1:100,000).

Hartono U, Baharuddin, Brata K. 1992. Geological map of the Madiun Quadrangle, Java (1:100,000).

Kadar D, Sudijono, 1993. Geological map of the Rembang Quadrangle, Java (1:100,000).

Koesmono M, Kusnama, Suwarna N, 1996. Geological map of the Sindangbarang and Bandarwaru Quadrangles, Java (1:100,000).

Koesoemadinata S, Noya Y, Kadarisman D, 1994. Geological map of the Ruteng Quadrangle, Nusatenggara (1:250,000).

Pendowo B, Samodra H, 1997. Geological map of the Besuki Quadrangle, Java (1:100,000).

Pringgoprawiro H, Sukido, 1992. Geological map of the Bojonegoro Quadrangle, East Java (1:100,000).

Purbo-Hadiwidjojo MM, Samodra H, Amin TC, 1998. Geological map of the Bali Sheet, Nusatenggara (1:250,000).

Ratman N, Yasin A, 1978. Geological map of the Komodo Quadrangle, Nusatenggara (1:250,000).

Rusmana E, Suwitodirdjo K, Suharsono, 1991. Geological map of the Serang Quadrangle, Java (1:100,000).

Santosa S, 1991. Geological map of the Anyer Quadrangle, West Java (1:100,000).

Santosa S, Atmawinata S, 1992. Geological map of the Kediri Quadrangle, Java (1:100,000).

Santosa S, Suwarti T, 1992. Geological map of the Malang Quadrangle, Java (1:100:000).

Sidarto, Suwarti T, Sudana D, 1993. Geological map of the Banyuwangi Quadrangle, Java (1:100,000).

Silitonga PH, 1973. Geological map of the Bandung Quadrangle, Java (1:100,000).

Sudjatmiko, 1972. Geological map of the Cianjur Quadrangle, Java (1:100,000).

Sudradjat A, Andi Mangga S, Suwarna N, 1998. Geological map of the Sumbawa Quadrangle, Nusatenggara (1:250,000).

Suharsono, Suwarti T, 1992. Geological map of the Probolinggo Quadrangle, Java (1:100:000).

Sujanto, Hadisantono R, Kusnama, Chaniago R, Baharuddin R, 1992. Geological map of the Turen Quadrangle, Java (1:100:000).

Sukamto R, 1975. Geological map of the Jampang and Balekambang Quadrangles, Java (1:100,000).

Suwarti T, Wikarno R, 1992. Geological map of the Kudus Quadrangle, Java (1:100,000).

Thanden RE, Sumadirdja H, Richards PW, Sutisna K, Amin TC, 1996, Geological map of the Magelang and Semarang sheets, Java.

Supplementary Material B – Spatial Database of Volcanic Features

Details of all volcanic vents identified on SRTM data and verified by published geological maps (Supplementary Material A) as part of this study. Vents are listed from east to west along the Sunda Arc, and the largest approximate diameter of the topographic feature, as measured from SRTM, is given (note for asymmetric features an average diameter is used). Only those structures with a diameter >3 km and of Quaternary age are listed (see text for details). Any vent that did not have a unique name was given the name of the topographic high which it either forms or occurs upon or, if no such name could be found, is unnamed.

Notes:

[1] These vents are known to be of differing chemistry/setting to the majority of volcanics, and the reference providing such information is given. They are discussed individually in section 3.2 of the main text.

[2] Indicates vents discussed in section 5 of the main text.

Vent/Caldera Name	Diameter /km	Coordinates - Decimal Degrees (WGS 1984)		Coordinates /m - UTM Zone 48S (WGS 1984)		Reference[1]
		Longitude	Latitude	Easting	Northing	
Krakatau	7	105.42255	-6.10135	546756	9325574	
Pulau Sebesi	6	105.48529	-5.94941	553712	9342364	
Congcot	7	105.86464	-6.27296	595644	9306543	
Tukung	7	105.93558	-6.11621	603522	9323860	
Aseupan	8	105.93615	-6.28783	603552	9304885	
Danau Caldera	12	105.96793	-6.18359	607089	9316404	
Pulosari	6	105.97798	-6.34192	608168	9298897	
Parakasak	6	105.98106	-6.24750	608528	9309335	
Kedepel	11	106.04479	-5.93359	615647	9344028	
Karang	12	106.04675	-6.27207	615791	9306605	
Perbakti	5	106.69325	-6.75105	687145	9253446	

Salak	15	106.73182	-6.70778	691426	9258216	
Pangrango	28	106.96260	-6.76949	716918	9251295	
Gede	28	106.98549	-6.79135	719438	9248866	
Kendeng	16	107.29179	-7.10829	753138	9213653	
Patuha	17	107.40582	-7.17624	765701	9206071	
Tangkuban Perahu	14	107.60661	-6.75916	788145	9252103	
Malabar	16	107.62248	-7.13614	789670	9210377	
Kendang	12	107.72005	-7.23036	800393	9199888	
Papandayan	13	107.72860	-7.32100	801277	9189851	
Manglayang	5	107.74327	-6.87662	803189	9239021	
Guntur[2]	7	107.84172	-7.14619	813898	9209122	
Cikuray	14	107.86321	-7.32407	816149	9189419	
Kareumbi	9	107.87881	-6.92932	818147	9233100	
Tampomas	13	107.96206	-6.76323	827468	9251428	
Kracak-Puncakgede[2]	12	107.97627	-7.26580	828687	9195787	
Sadakeling[2]	10	108.03244	-7.11528	835006	9212409	
Galunggung Calderas[2]	13	108.06857	-7.22880	838917	9199815	
Cakrabuana	16	108.13256	-7.04358	846130	9220273	
Sawal[2]	16	108.26299	-7.19804	860437	9203071	
Cereme	20	108.40763	-6.89496	876676	9236518	
Slamet	26	109.21643	-7.24176	965875	9197362	
Dieng Volcanic Complex[2]	17	109.90233	-7.22424	1041850	9198542	
Sundoro[2]	20	109.99566	-7.29999	1052097	9190024	
Sumbing	27	110.07422	-7.38199	1060699	9180827	
Ungaran[2]	11	110.34350	-7.18850	1090791	9201958	
Telomoyo[2]	5	110.40252	-7.36045	1097106	9182790	
Merbabu[2]	30	110.43920	-7.45280	1101046	9172487	

Merapi	40	110.44720	-7.53889	1101815	9162916	
Muria[1]	40	110.87103	-6.61839	1150090	9264587	Nicholls & Whitford (1983); Leterrier et al. (1990)
Genuk[1]	5	110.92559	-6.45022	1156372	9283203	
Djobolarangan	45	111.18458	-7.69423	1183323	9144553	
Lawu	32	111.19322	-7.62558	1184392	9152172	
Lasem[1]	9	111.51861	-6.68288	1221989	9256512	Bello et al. (1989); Leterrier et al. (1990)
Patukbanteng	13	111.65668	-7.79825	1235522	9132189	
Wilis	44	111.76030	-7.81224	1246998	9130448	
Pandan[2]	7	111.79863	-7.45999	1251874	9169588	
Kelud	19	112.30824	-7.93608	1307610	9115628	
Kawi	11	112.44311	-7.92113	1322625	9117026	
Boklorobubn	25	112.44781	-7.76660	1323455	9134242	
Butak	26	112.47147	-7.95337	1325712	9113376	
Arjuno-Welirang	23	112.58948	-7.76481	1339210	9134160	
Penanggungan	8	112.61970	-7.61482	1342871	9150824	
Buring	6	112.67915	-8.02052	1348655	9105462	
Semeru	24	112.92187	-8.10905	1375450	9095068	
Tengger Caldera	37	112.95054	-7.95043	1378984	9112706	
Lamongan	7	113.34044	-7.98080	1422310	9108454	
Iyang-Argapura	37	113.59521	-7.97552	1450699	9108458	
Ringgit[1]	7	113.85551	-7.72144	1480315	9136257	Edwards et al. (1994); Leterrier et al. (1990)
Raung	28	114.05485	-8.11952	1501581	9091240	
Rante	10	114.21455	-8.09622	1519453	9093444	
Ijen-Merapi	20	114.25816	-8.06468	1524399	9096864	
Baluran[1]	11	114.37113	-7.84059	1537581	9121671	Leterrier et al. (1990)
Kelatakan	7	114.49619	-8.20359	1550601	9080686	

Merbuk	17	114.64956	-8.22589	1567663	9077773	
Pata	13	114.81643	-8.25986	1586206	9073507	
Batukau	17	115.08751	-8.33555	1616282	9064249	
Bratan	23	115.13854	-8.26209	1622199	9072347	
Batur	37	115.37734	-8.23808	1648980	9074349	
Agung	20	115.50722	-8.34278	1663202	9062200	
Seraja	11	115.65634	-8.38085	1679777	9057467	
Rinjani	40	116.41330	-8.40868	1764534	9051919	
Nangi	30	116.56103	-8.41348	1781100	9050884	
Sangenges[1]	25	117.11504	-8.56363	1842827	9032011	Foden and Varne (1980)
Tambora[1]	40	117.99207	-8.24623	1942822	9064711	Foden and Varne (1980); Foden (1986)
Tarowa (D. Tanah Merah)	14	118.15805	-8.70485	1959778	9012070	
Labumbu	21	118.19285	-8.42284	1964822	9043920	
Matlia (D. Matua)	12	118.41035	-8.38772	1989539	9047056	
Lambuwa	13	118.48010	-8.34780	1997584	9051315	
Doro Pokah	28	118.55948	-8.40441	2006338	9044569	
Doro Kolo	10	118.74404	-8.39031	2027281	9045431	
Doro Maria	23	118.90911	-8.48066	2045603	9034481	
Sangeang Api[1]	15	119.06416	-8.19198	2064363	9066700	Foden and Varne (1980)
Doro Saboke	7	119.11759	-8.68052	2068370	9010855	
Gili Banta	7	119.29218	-8.40521	2089345	9041469	
Doro Otota	7	119.40895	-8.71108	2101265	9006103	
Doro Ora	13	119.66369	-8.75461	2129976	9000000	
Gunung Wajor	6	119.92088	-8.77318	2159106	8996704	
Unnamed Caldera	10	119.92807	-8.66238	2160435	9009330	
Gunung Beliling	10	119.96500	-8.62738	2164795	9013161	

Wai Sano	21	119.99006	-8.71187	2167255	9003390	
Poco Dedeng	19	120.02134	-8.75795	2170598	8997978	
Peg. Todo	21	120.28497	-8.75931	2200587	8996585	
Peg. Pocokuwus	8	120.30485	-8.59908	2203607	9014830	
Poco Mandasawu	11	120.42157	-8.64124	2216707	9009455	
Poco Leok (Likong)	16	120.47232	-8.71262	2222150	9001039	
Ranakah	10	120.50432	-8.64466	2226122	9008671	
Poco Ndeki	5	120.64015	-8.83037	2240707	8986735	
Watuweri	7	120.73428	-8.72088	2251981	8998828	
Unnamed vent	9	120.74336	-8.84368	2252410	8984700	
Unnamed vent	18	120.94468	-8.76463	2275781	8992772	
Inerie	11	120.95402	-8.87714	2276281	8979809	
Inielika	8	120.97447	-8.72069	2279402	8997668	
Ebulobo (W. Ambulombo)	11	121.19035	-8.81608	2303588	8985627	
Keli Lambo	6	121.29741	-8.65343	2316660	9003782	
Keli Kotto	9	121.32178	-8.87117	2318331	8978619	
Unnamed vent	8	121.32252	-8.75250	2319029	8992262	